Proc. of SPIE Vol. 1113, Reflective Optics II, ed. D G Korsch (Oct 1989) Copyright SPIE

Design of a Catadioptric Lens for Long-Range Oblique Aerial Reconnaissance

James J. Ulmes
Research and Engineering

CAI, a Division of RECON/OPTICAL, INC.
550 W. Northwest Highway
Barrington, IL 60010

ABSTRACT

The design of a lens for long-range oblique aerial reconnaissance demonstrates how lightweight reflective optics are effective in producing an optical system which can detect, recognize, and identify distant ground objects from an airborne platform. The lens herein described transforms an object space filled with low-contrast targets of small angular subtense to an image space having the spatial and optical characteristics best suited to an electro-optical detector designed for this application. The lens incorporates two key reflective elements: a lightweight primary mirror which provides all the optical power of the lens, and a scan mirror of cellular construction which directs light into the lens.

Although the nominal design is diffraction limited, the scan mirror deflections caused by gravity induce notable wavefront errors. Finite element techniques were used to predict the deflections. The deflections were then used to predict lens performance.

The lens has been built and tested, and test results agree with predictions. The lens/detector-system combination allows intelligence gathering from an airborne platform at standoff ranges up to 150 nmi.

1. INTRODUCTION

Modern tactical reconnaissance requires that aircraft obtain imagery at increasingly long distances from the target to avoid the improving capabilities of ground-based defenses. This presents some new challenges for sensor design. The dimensions to be resolved on the target are constant, but they subtend smaller angles in a sensor's field of view because of the increased distance to the target. The airpath between the sensor and the target reduces the apparent contrast at the entrance pupil considerably. The atmosphere absorbs or scatters certain wavelengths and alters the spectral composition of the light coming from the target.

To provide a sensor that will perform in this environment, a reconnaissance system has been developed which includes a camera, a data transmission system, and an image exploitation system. This paper focuses on the lens characteristics which allow it to transform the given object space to an image space best suited for the detection and exploitation systems. As with all lens designs, some consideration must first be given to the important aspects of the object space and to the desired characteristics of the image space.

As shown in figure 1, aerial reconnaissance sensors are typically required to resolve 3 to 20-ft dimensions at distances of 50 to 150 nmi. The corresponding span of angular subtense is 10 to 22 μrad (2 to 5 seconds of arc). (For reference, the field of view will be roughly 60 mrad; i.e., 3.4°.) The apparent target contrast at the sensor entrance pupil will range from 2:1 to 1.03:1.

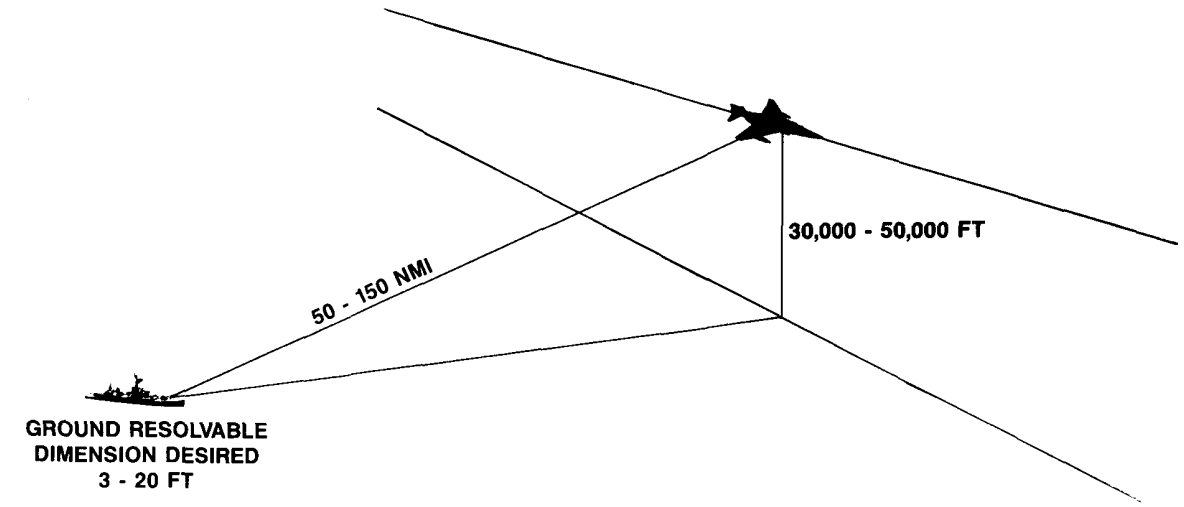

Figure 1 Long Range Oblique Reconnaissance

The detector determines what the image characteristics should be. The device used in this reconnaissance system was developed specifically for this application and is shown in figures 2 and 3. The detector, a silicon-based Charge Coupled Device (CCD), is a linear device. The scene is scanned line-by-line as the image is moved past the array of pixels. (The entire sensor body rotates to cause this image motion.)

The 11 by 11- μm pixel size affords adequate response to the illuminances to be encountered, and is compatible with the desired ground-resolvable dimensions (given a proper lens).

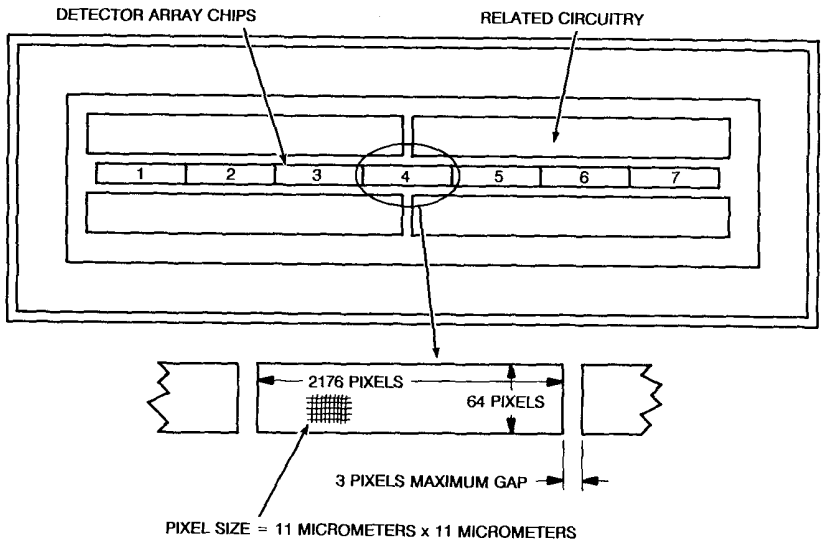

Figure 2 Focal Plane Array Schematic

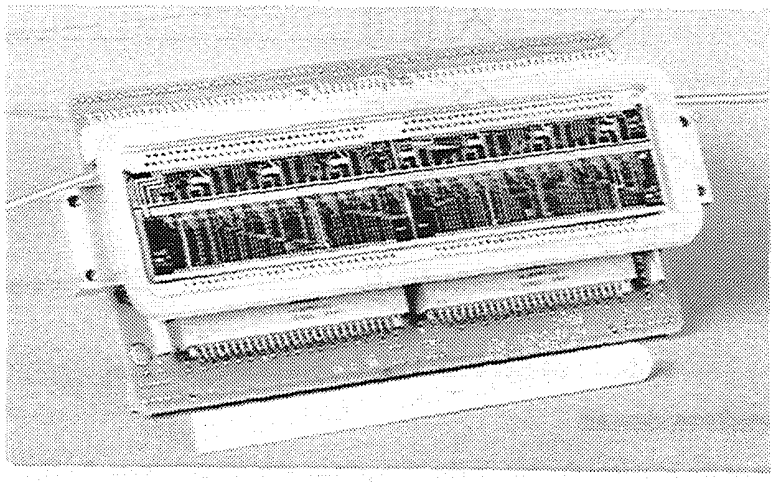

Figure 3 Focal Plane Array

Compared to film, the CCD is an optically slow detector. It must be exposed roughly three times longer than film for a given illuminance. Exposure is controlled by passing the charge from one row of pixels to another, up to 64 times, depending on light conditions.

The spectral range of a CCD is broader than that of film. Typically, high-resolution film does not respond well at wavelengths beyond 700 nm. The CCD will respond to wavelengths up to 850 nm. This is advantageous because the longer wavelengths penetrate the atmosphere better, affording improved apparent entrance pupil contrasts to the sensor.

Each pixel in the detector array has a unique sensitivity to light. The nonuniformities are measured as the entire array is illuminated by a diffused and uniform source, and compensation is made in the image processing chain for these variations. Additionally, in the image processing chain, contrast is enhanced by subtracting the background luminance. By implication, the lens should have minimal variation in relative illumination across the field, and there should be protection against stray light and veiling glare.

Because this system is to be flown on an aircraft, minimum weight is a prime consideration. The strength of the assembled system and the individual components must be adequate to survive various severe loading conditions, including a shock load of 12 g's.

From the above considerations of object space, image space, and operational environment arise the following performance criteria for the lens.

- The lens should have a focal length adequate to achieve the desired ground-resolvable dimensions given the detector pixel size.
- The lens must provide good image illuminance because the detector is optically slow.
- The lens must be well corrected to preserve modulation because the apparent entrance pupil contrasts are low. This correction must be achieved over a wide spectral range because the detector has a wide spectral response.
- The lens must have uniform relative illumination across the field and must be protected against stray light and veiling glare.
- The lens must be lightweight to be airborne, and its components must be strong enough to withstand aircraft loading.

2. THE SLOTTED CATADIOPTRIC LENS DESIGN

A lens which meets the above criteria is shown in figure 4. It is a 110-inch focal length, f/5.6 catadioptric system. The scan mirror directs light from the target into the lens. The light bundle passes through two refractive elements (the aperture correctors) to a spherical primary mirror, the source of all power in the lens. The converging beam passes through the aperture correctors and through a slot in the scan mirror to a refractive pair of field correctors. The light bundle then passes through a pair of wedges whose relative motion keeps the image focused on the detector. Before reaching the surface of the detector, the light passes through spectral filters which tailor the spectral content of the image to that best suited to system performance.

The lens elements are housed in a sensor body made of a graphite-epoxy composite. The body has a zero coefficient of thermal expansion along the optical axis, rigidity sufficient to assure alignment during operation, and a first natural frequency above 200 Hz.

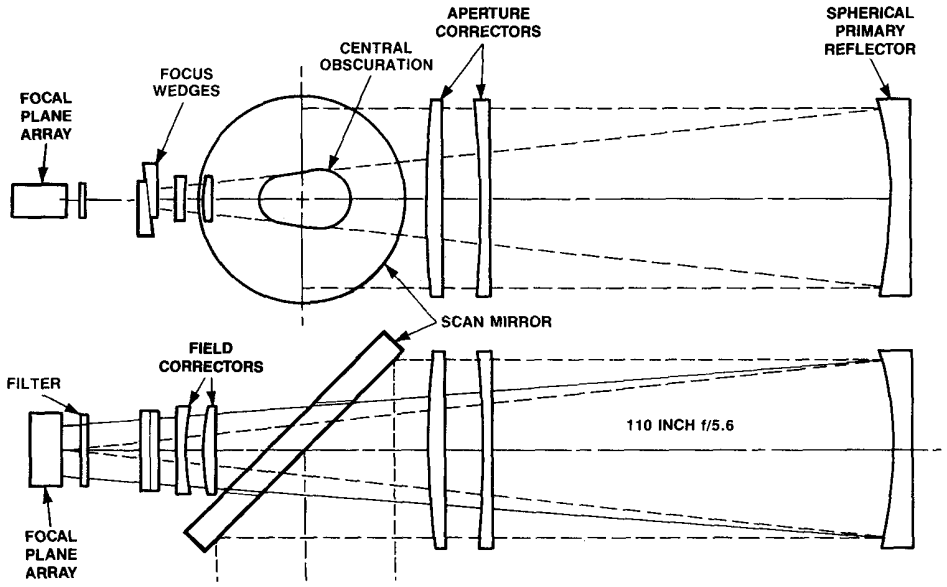

Figure 4 110-inch Focal Length, f/5.6 Catadioptric Lens

2.1. Functions of the lens constituent elements

The scan mirror, which directs the light into the lens, is also the aperture stop for the system. Its asymmetric slot creates a 13 percent obscuration. Because it is nominally oriented at 45° to the optical axis, it is the largest element in the lens and therefore presents the largest challenge in optomechanical design.

The aperture correctors remove the spherical aberration associated with the spherical primary. Because all the optical power for the lens is in the primary, the correctors do not contribute significant chromatic aberration, nor do they induce any substantial spherochromatism. All surfaces of the aperture correctors are spherical and are suited to conventional manufacture and inspection.

The field correctors correct for coma, astigmatism, and field curvature. They are located close to the image plane to avoid chromatic aberration. These correctors allow for the 3.4° field of view to be imaged to a 6.60-inch wide focal plane with less than .0002 inch deviation from flatness.

The focusing wedges are a pair of opposed prisms which together constitute a flat plate in the optical path. Their relative motion changes the thickness of this flat plate and adjusts the image location in mechanical space. They are servo-controlled and maintain image focus on the detector within .00025 inch despite changes in range, temperature, or pressure.

A Schott 06-515 filter for blue subtraction and a cutoff filter for wavelengths above 850 nm are used to preserve the high degree of lens correction.

2.2. Lens performance

The lens design is diffraction-limited as shown by the Modulation Transfer Function (MTF) plot of figure 5.

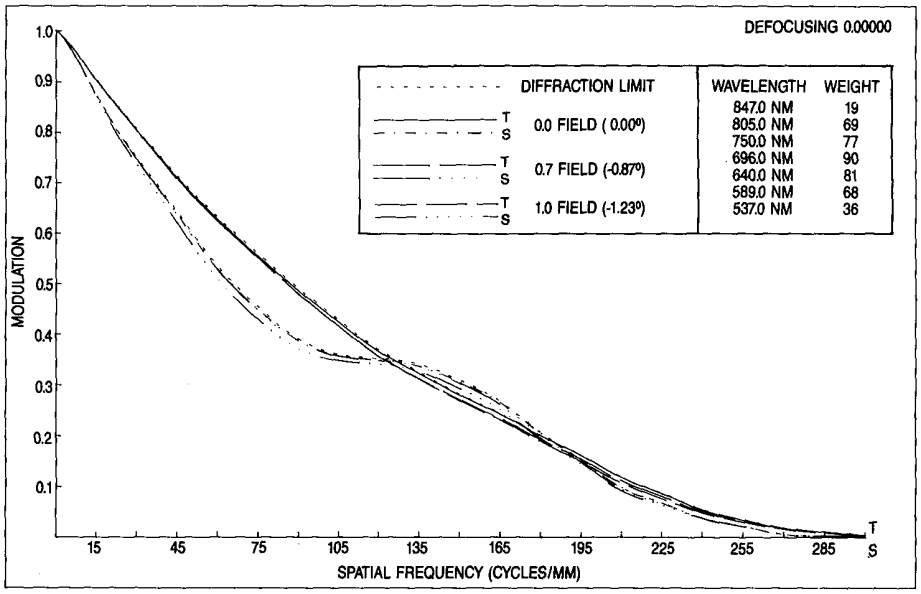

Figure 5 Nominal Catadioptric Lens MTF

Taking into account the 13 percent obscuration, a 4 percent loss due to trimming the scan mirror ellipse at the edges, and the glass and coatings used, the lens has a T-number of 7.3.

Relative illumination varies by only 0.9 percent across the field of view. The location of the focal plane behind the scan mirror provides an intrinsic shield against stray light.

Actual lens performance is somewhat different than that of the nominal design because of the structural deformations of the reflective elements (particularly the scan mirror). The optomechanical design and analysis of these elements will be considered in detail before examining the performance of the actual lens.

3. THE SCAN MIRROR

The scan mirror represents a design challenge in lightweight reflective optics. The optical surface approximates an ellipse with axes of 29.50 and 20.30 inches; some truncation of the ellipse occurs at the edges to reduce the major mechanical dimensions to 28.75 by 18.50 inches (see figure 6). This mirror is unusually large for an aerial reconnaissance system. Although space-based optical systems involve larger mirrors, such mirrors are weightless when in use. This mirror has to be ultralightweight to be part of an airborne system, yet has to maintain optical quality while being operated in a gravity field and in a wide range of orientations. The mirror is used for azimuthal pointing of the sensor and is driven to compensate for the relative motion of the aircraft and the target, so the rotational inertia had to be as low as possible. Finally, to ensure dependable performance, the lowest natural frequency of the mirror in its mount had to exceed 200 Hz.

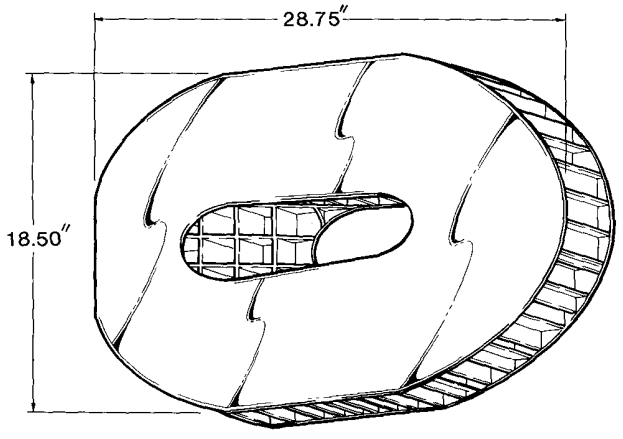

Figure 6 Scan Mirror

3.1. Scan mirror slot

The slot for the converging ray bundle exerts a dominant influence on the mirror's optical and mechanical performance. The slot is an unusual shape because the detector is a linear array and the mirror is inclined with respect to the converging ray bundle. The slot has a gradual taper and elliptical ends. The overall length of the slot on the optical surface is 14.38 inches, the maximum width is 4.34 inches, and the width at the start of the ellipse on the narrow end is 3.68 inches.

The slot is asymmetrically located on the optical surface because of the mirror's inclination along the optical axis. This inclination also causes the slot to project obliquely with respect to the mirror surface into the mirror body.

3.2. Scan mirror construction

The scan mirror is made of Corning Glass ULE titanium silicate and has a construction of a cellular core sandwiched between thin front and back plates. The cells are 1.50 inches square and have .080-inch thick glass walls. At the corners of each cell are .150-inch square glass struts. The mirror is 4.550 inches thick, of which .200 inch is the front plate (the mirrored surface) and .150 inch is the back plate (the site of the mount attachment points).

The pieces of the scan mirror were joined together by fusing and frit-bonding. The mirror surface was ground and polished on a continuous grinding machine. On a root-mean-squared (rms) basis, surface figure error was held below .021 wavelength (the reference wavelength being 632.8 nm), and quilting effects (the pass through of the cellular core pattern to the mirrored surface) were held to .004 wavelength rms.

The coating applied to the scan mirror is an aluminum-silicon monoxide system designed to have maximum reflectance at 45°. It has an average reflectance of 90 percent or better in the region from 520 to 700 nm, and 88 percent or better from 700 to 850 nm.

The scan mirror rear surface is also coated to avoid asymmetry in coating-related stresses.

3.3. Scan mirror mounting

The structural deformation of the scan mirror under load is as much dependent upon its mount as upon its construction. The mount is shown in figure 7. The design avoids generation of strains due to overconstraint of the mirror and provides, in effect, a three-point mount.

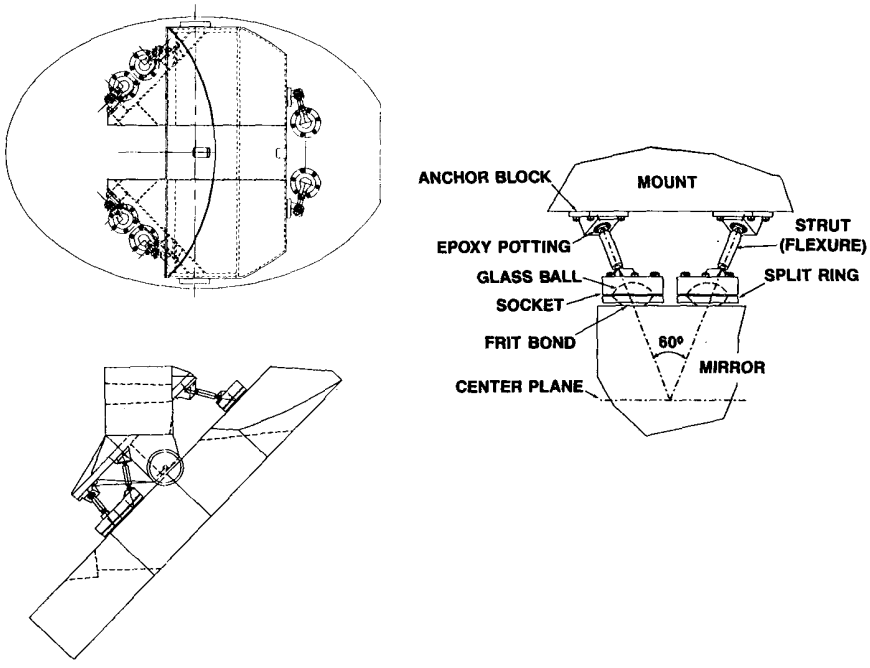

Figure 7 Scan Mirror Mounting Structure

The mirror is held to a yoke by three pairs of struts. Each strut is attached to the back plate of the mirror with a ball joint. The struts are weak in bending and act primarily in simple tension or compression.

The two struts in each pair are oriented so that their axes intersect at a point on the mirror's neutral bending axis. Thus, although there are six attachment points to the mirror, there are effectively three mounting points. Because there are six struts acting effectively as uniaxial elements, all six degrees of freedom are constrained without the introduction of localized bending strains.

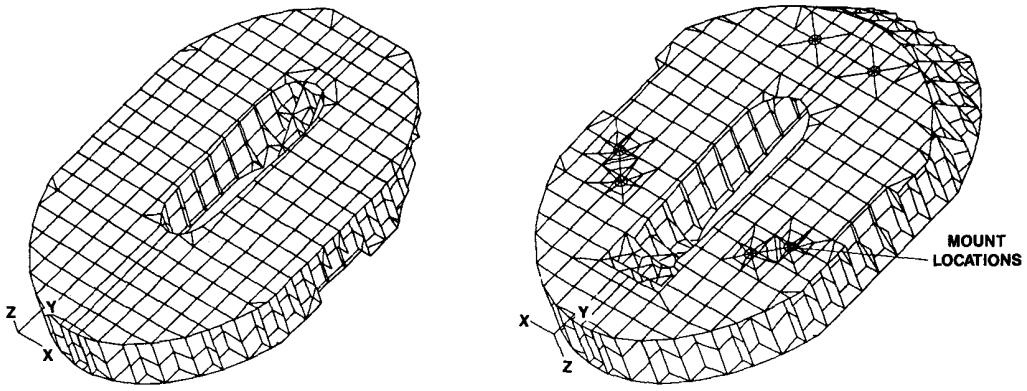

Figure 8 Scan Mirror Finite Element Model

3.4. Scan mirror deflection analysis

To anticipate structural deformations of the mirror, a finite-element model was created as shown in figure 8, using NASTRAN from the MacNeal-Schwendler Corporation. The predicted surface deformation at 30° depression and 1 g is shown in figure 9. This surface deformation approximates a trefoil shape, and lens performance was predicted by introducing a trefoil aberration, described by Zernike coefficients, into a computer model of the lens. A wavefront with the desired aberrations was created at the lens entrance pupil; all remaining components remained as designed. The analysis was performed using the Code V program from Optical Research Associates.

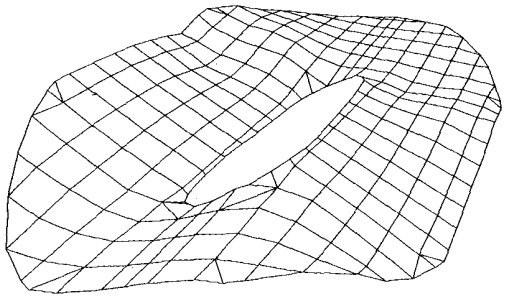

Figure 9 Predicted Scan Mirror Surface Deformation Under Gravity Loading

The actual surface deformation of the mirror was measured by interferometry and is shown in figure 10. This measured shape correlates well with the one predicted by the finite-element method. The interferometric data was translated into a grid of optical path differences across the aperture and used to create a measured, aberrated wavefront at the lens entrance pupil in the computer optical model. The resultant lens performance predictions were close to those obtained with the Zernike approximation of the surface deformation.

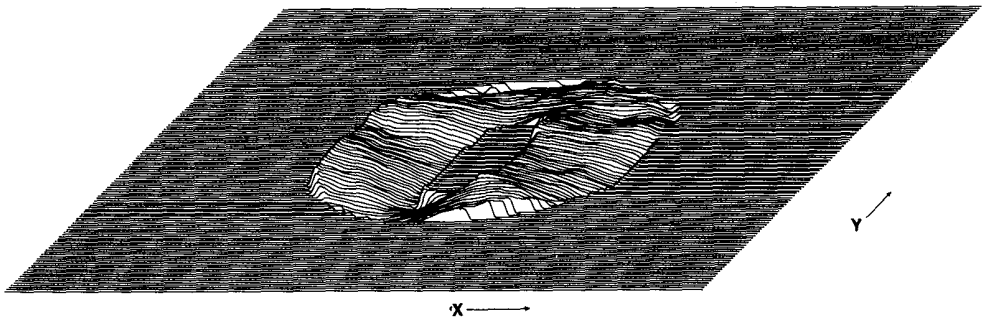

Figure 10 Actual Scan Mirror Surface Deformation Under Gravity

In both the finite-element model and in the mirror interferometry, the combined effect of the slot and the mount is evident in the shape of the mirror distortion. The slot causes a discontinuity in stiffness, and the support configuration causes the two halves of the mirror (above and below the slot) to move in a louver-like fashion. Such a shape has large coefficients associated with the trefoil term in Zernike polynomials, although coefficients associated with other aberrations are also necessary to fully characterize such a shape.

3.5. Natural frequency of the scan mirror, mount and yoke

Finite element analysis was also used to predict the first (lowest) natural frequency of the mounted mirror. The mirror, the mounting struts, and the yoke used to install the entire assembly into the sensor were included in the model. A first modal frequency above 200 Hz, the design requirement, was achieved. A significant challenge in achieving this was accomplishing a compromise between two goals: maximum stiffness of the support struts for high natural frequency; and flexibility in those same struts to avoid input of yoke strains (particularly thermal ones) to the mirror.

3.6. Importance of analysis to the scan mirror design

The deformed scan mirror makes the largest contribution to the total aberration in the real lens. Without a prediction of the surface deformations by analytical methods before fabrication, the lens performance would have been seriously overestimated, and tolerances on other image-degrading factors would have been mistakenly loosened. Such an analysis was essential to providing a lens meeting system requirements.

As is the case with such large, extremely lightweight optical components, the mechanical analysis directs and constrains the component design, and cannot be implemented only as a follow-on check.

4. THE PRIMARY MIRROR

4.1. Primary mirror construction

Because all lens optical power resides in the primary mirror, it is critical that this mirror have good surface figure. Two factors can affect the surface figure: the quality of manufacture, and the strain induced or inherent in the mirror.

Quality in manufacture was assured by using a spherical surface in the design. Such a surface is accurately made and inspected by conventional techniques.

The prime challenge in the design of the primary mirror is the achievement of maximum resistance to strain with minimum weight. This was also the case with the scan mirror; however, the primary mirror, which is round and 23 inches in diameter, is not as large as the scan mirror. A conventional, solid piece of glass is used, but it is lightened by removal of material. As shown in figures 11 and 12, the glass blank has several 2.00-inch diameter holes drilled in it. These holes are centered on the neutral bending axis of the piece to maintain its bending strength despite the loss of material.

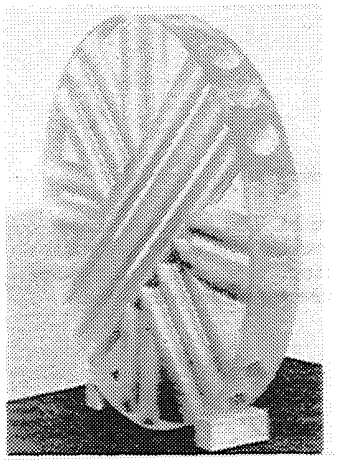

Figure 11 Primary Mirror

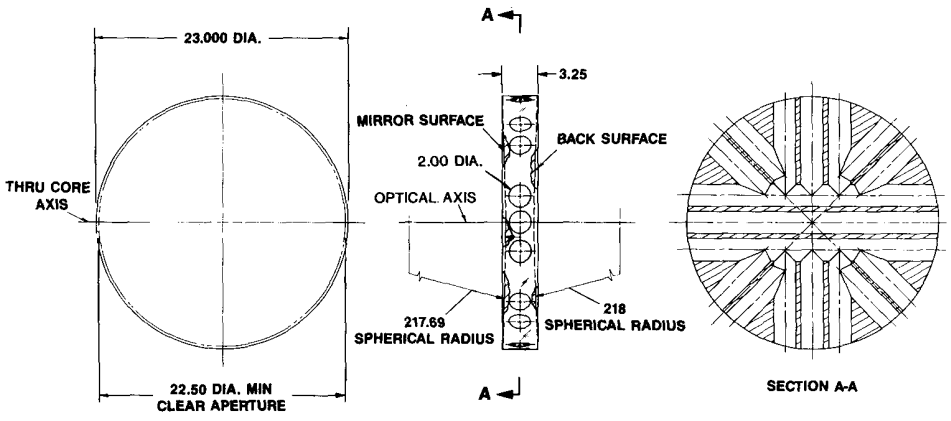

Figure 12 Cored Glass Blank for Primary Mirror

The mirror is symmetrical in several respects, but in particular with respect to the bending axis. The same radius of curvature is ground on the back face as on the front, and both front and back surfaces are coated. This symmetry provides uniformity of response to manufacturing-induced and residual stresses.

The mirror is made of Corning ULE titanium silicate. The coating is enhanced aluminum with a multilayer dielectric overcoat. It is designed to have better than 88 percent reflectivity over the entire spectral range of interest.

A prediction of the surface deformation under gravity load was required early in the design effort. This was done because it was not known if a perfectly made part would demonstrate proper figure on a test stand. A finite element model of this mirror was created and is shown in figure 13. This model was more challenging than that of the scan mirror. Solid elements (rather than plate elements) had to be used in a geometry that was complex by virtue of the intersection of several solid sections with each other (the cores with each other and with the blank having two spherical surfaces). Because of symmetry, only a fraction of the entire mirror had to be modeled.

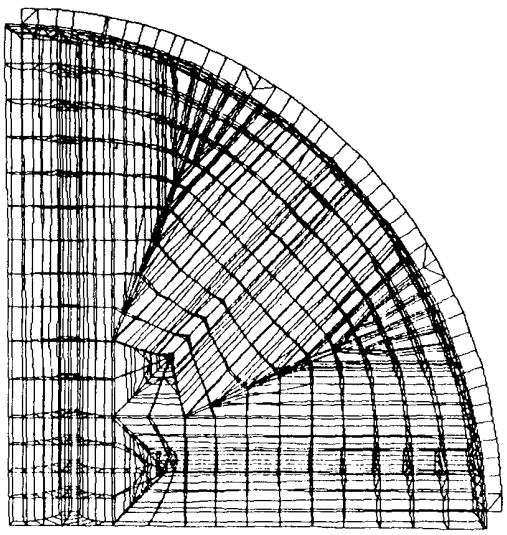

Figure 13 Primary Mirror Finite Element Model

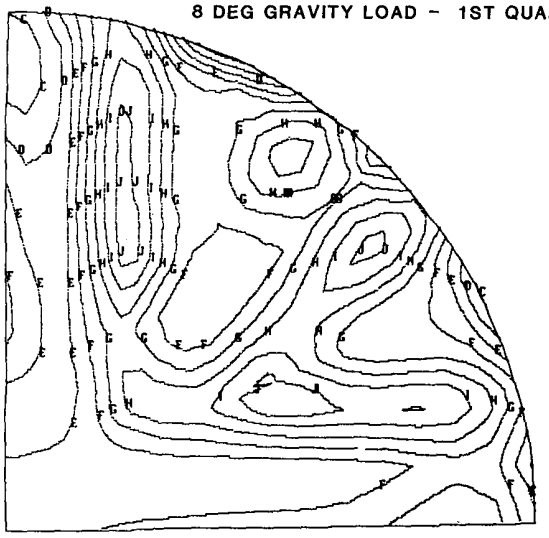

Figure 14 Primary Mirror Surface Deformations Predicted by Finite Element Model

A sample of the predicted deformation of the primary mirror under load is shown in figure 14. The deformation pattern reflects the presence of the cores, but the magnitudes are on the order of .0008 wave per contour increment. Zernike polynomial coefficients and rms wavefront error were calculated and used to evaluate the effect of the deformation on system performance.

4.2. Primary mirror mount

The primary mirror mount is the pathway through which external forces exert stresses on the mirror, and it establishes the boundary conditions relevant to mechanical analysis. In this case, the mount is heavily constrained by its allowed geometrical envelope. The mirror mount cannot extend more than 1 inch radially beyond the mirror, nor can it increase the overall length of the sensor. In addition, the structural integrity of the sensor body has to be maintained, so the mount has to allow assemblies on either side of the mirror to be directly joined together.

The mount design is shown in figure 15. The mirror is mounted in a thin ring of a steel alloy with a low coefficient of thermal expansion. The mirror is attached to this ring by pads of Room-Temperature-Vulcanizing (RTV) silicone rubber. Three flanges of approximately 20^0 subtense extend beyond the ring to provide the attachment points to the sensor body. (These attachment points are discrete ears rather than a continuous ring because of considerations encountered in maintaining the structural strength and continuity of the sensor body.)

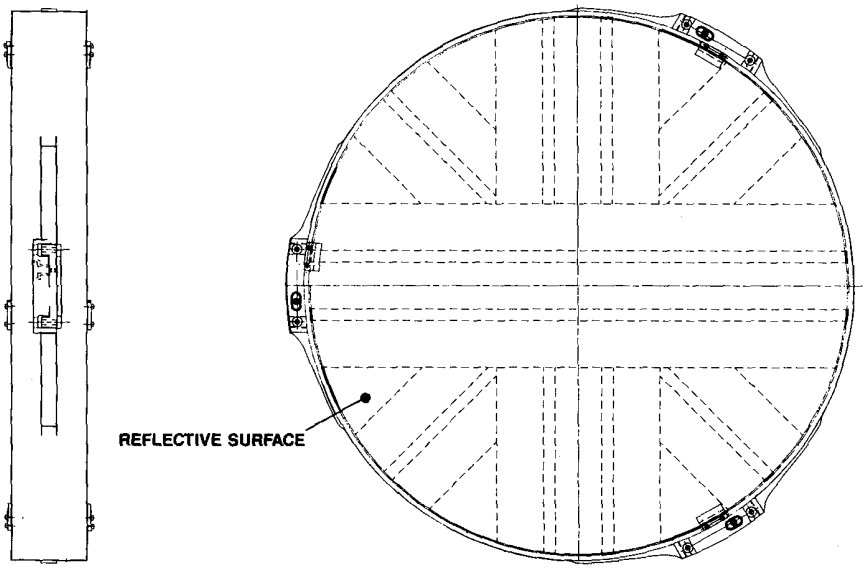

Figure 15 Primary Mirror Mount Design

A finite element model of the mount was added to that of the mirror, and various mounting disturbances (such as temperature changes and attachment point strains) were applied. The thickness, number, and location of the RTV pads were varied to achieve minimum sensitivity to the disturbances.

A constraint on the mounted mirror is that its first modal frequency must be above 200 Hz. The bezel is not rigid, so finite element methodology is needed to predict this quantity. As shown in figure 16, the first mode resembles that of a drum or piston, with displacement occurring primarily along the optical axis. It was found that, with the original design, this mode would have occurred at a frequency below 200 Hz. Some clips were added to the front and back sides of the mount to stiffen it, and the frequency increased above the specified minimum.

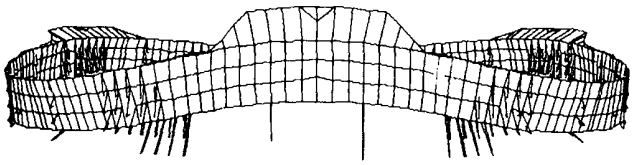

Figure 16 Primary Mirror Mount Fundamental Vibration Mode Prediction

The mirror has been mounted and inspected in a variety of orientations, and has shown a surface figure of .10 wavelength peak-to-valley or better.

5. ACTUAL LENS PERFORMANCE

The lens has been assembled, and interferometry of the entire system has been taken. The MTF curve shown in figure 17 was computed from this interferometry. This data incorporates all wavefront aberrations and alignment errors in the actual system. The result correlates well with a prediction made using the deformations indicated by finite element analysis.

To assess the relative merit of the lens performance, the curve of figure 17 was replotted (figure 18) showing the MTF as a function of angular frequency in the object space. In this way, lens performance for several combinations of ground-resolvable dimensions and standoff ranges can be readily identified. In addition, the performance of this lens can be compared to another lens of different focal length already used in aerial reconnaissance. This other lens, a 66-inch, f/5.6 refractor used in film cameras, is highly regarded for its excellent performance and high-quality photographic imagery.

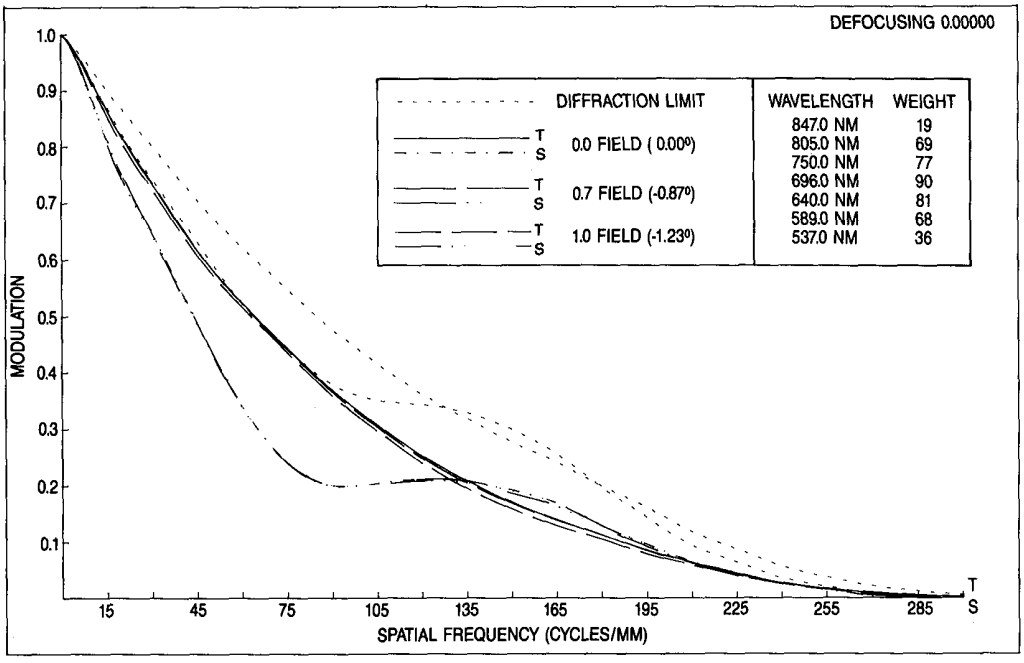

Figure 17 Actual Catadioptric Lens MTF

Examination of the two curves of figure 18 indicates that the catadioptric lens offers a substantial advantage in MTF for any target in the object space. The longer focal length also offers the ability to resolve smaller targets before the detector's Nyquist frequency (the frequency established by the pixel-to-pixel spacing) is exceeded.

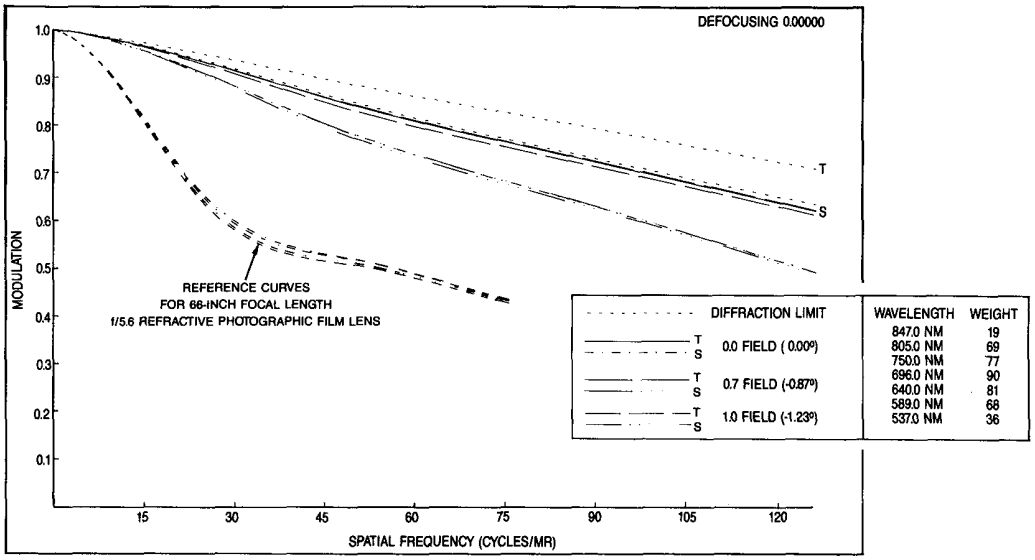

Figure 18 Actual Catadioptric Lens MTF as a Function of Angular Frequency in Object Space

6. SYSTEM PERFORMANCE

The lens is one element of the reconnaissance system. The lens is successful if its characteristics are matched to other system elements and its limitations are held within the budgeted tolerances. The success of the lens design and manufacture is indicated by the system performance curve shown in figure 19. (The conditions indicated are representative of what will be encountered on reconnaissance missions.) Here again, to serve as a basis for reference, the airborne performance of a system with a 66-inch focal length, refractive lens is shown for comparison. The superior performance of the sensor with the catadioptric lens affords typically an additional 20 nmi of standoff range from a target for the same ground-resolvable dimension. The performance confirms the approaches taken in the lens and system design, and shows that the system will deliver critical tactical intelligence from survivable ranges.

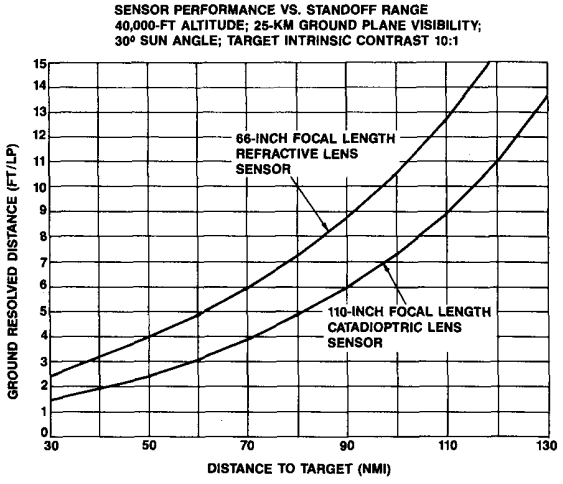

Figure 19 Anticipated Airborne Performance of Complete Reconnaissance System

7. CONCLUSIONS

Mechanical deformation analysis is critical in the design of lightweight reflective components. Mechanical strains in mirrors can significantly alter lens performance. Finite element analysis can be used to predict surface deformations. These wavefront disturbances should be included in the lens optical analysis to establish performance predictions and tolerances for components and subsystems.

A consequence of the importance of the analysis is that it cannot be implemented merely as check on a component design. It will determine many aspects of that design.

Interferometric inspection of components should be used to check analytical predictions of surface deformation. This information can also be used to more accurately predict lens performance in advance of assembly.